Geotechnical Engineering

Measuring horizontal stresses during jacked pile installation

--Manuscript Draft--

Manuscript Number:	GE-D-14-00069R3
Article Type:	Theme - Construction Processes and Installation Effects
Corresponding Author:	Francesca Burali d'Arezzo Cambridge University Cambridge, Cambridgeshire UNITED KINGDOM
First Author:	Francesca Burali d'Arezzo
Order of Authors:	Francesca Burali d'Arezzo
	Stuart Kenneth Haigh
	Mark Talesnick
	Yukihiro Ishihara

- Date of last revision: 13th January 2015.
- Number of words: 5,219 (it does not include abstract and references)
- Number of figures: 10

Measuring horizontal stresses during jacked pile installation

Author 1

- Francesca Burali d'Arezzo, MEng
- Department of Engineering, Cambridge University, Cambridge, UK

Author 2

- Stuart Haigh, PhD
- Department of Engineering, Cambridge University, Cambridge, UK

Author 3

- Assoc. Prof. Mark Talesnick, DSc
- Faculty of Civil and Environmental Engineering, Technion-Israel Institute of Technology, Haifa, Israel

Author 4

- Mr. Yukihiro Ishihara, MEng
- Giken Ltd, Kochi, Japan

Full contact details of corresponding author.

Francesca Burali d'Arezzo fb379@cam.ac.uk

Abstract

Jacking is an installation technique for displacement piles commonly used onshore in urban environments owing to its low noise and vibration. During pile jacking, stress changes occur in the soil which are substantial close to the pile but also extend a significant radial distance. These stresses are difficult to measure accurately due to arching around stress sensors. In the field, stress measurements are commonly made by means of an adjacent pile whose stiffness changes the stress field within the soil. Accurate measurements of stresses due to installation of a single pile under laboratory conditions are needed in order to quantify this error.

In this paper, null-gauges that do not suffer from membrane deflection were used to measure horizontal stress changes during the jacked installation of a cylindrical pile in dry sand. Stresses were measured both by means of an adjacent pre-installed square pile and in-soil sensors. The paper also presents a comparison between the centrifuge results and the radial stress distribution estimated using conventional methods, such as Boussinesq's elastic analysis and elasto-plastic spherical cavity expansion.

Keywords chosen from ICE Publishing list

Piles & piling; Granular materials; Stress analysis.

List of notation

Roman letters

C_U	Coefficient of uniformity
D	Diameter of the cylindrical pile
D_{50}	Grain size at which 50% by mass of the sand is smaller
h	Height above the pile tip
K_a	Active coefficient of lateral earth pressure
p	Pressure at the cavity wall
q_b	Pile base stress

R Radius of the cylindrical pile

R_N Normalised roughness (Uesugi and Kishida, 1987)

x Horizontal distance between the cylindrical pile centreline and the outer face of the gauge

r Distance between the centre of the pile tip and the middle of the outer face of the gauge along the direction radial to the cavity sphere

W Width of square pile

Greek letters

ϕ' Friction angle

σ_1 Component of stress radial to the spherical cavity

σ_h Horizontal component of stress

θ Angle b the direction radial to the cavity sphere and the vertical

1. Introduction

Onshore piles can be installed using either displacement or non-displacement processes, both of which change the stress-field around the installed pile. These stress changes affect both the pile's own performance and the stresses exerted on surrounding structures or other piles within pile groups.

Displacement piles are forced into the ground either by a hammer during pile driving or by a static jacking force during pile jacking. During both of these processes, the soil is radially and vertically displaced to permit the pile penetration. The final stresses will therefore differ markedly from the free field in-situ stresses. While locked-in stresses are imposed around driven piles in all soil types, these are most significant for piles in sand (Poulos, 1987). As the stresses created in the soil during pile diving are significant, pile installation method has a substantial impact on a pile's vertical capacity.

In this paper, the stress field created during the installation of a jacked pile in sand will be examined using centrifuge modelling in which 1: N scale models are tested at Ng in order to give homologous stress fields in the model and prototype. Testing of piles within geotechnical centrifuges has a substantial history; Ko *et al.* (1984) first showed the importance of performing the pile installation in flight, in order to induce the correct stress-field within the soil surrounding the pile. The authors showed that the bearing capacity of a pile installed and tested in flight is 60% of that of the same pile installed at 1g and tested in flight. Results of piles installed at 1g should therefore be considered carefully.

A large amount of centrifuge and calibration chamber testing has also been performed to examine the penetration mechanism around cone penetrometers installed in sand. The mechanism is very similar to that of a penetrating pile, though care should be taken when extrapolating these results to model piles due to scaling effects. Bolton *et al.* (1999) analysed the scale effect due to the ratio between the pile diameter and the soil's grain size. The authors showed that similar values of cone resistance were recorded in fine and medium sands when

the ratio between the pile diameter and the sand's D_{50} grain size was larger than 20. This scale effect can be present for model tests both in centrifuges and in calibration chambers. Scale effects also exist due to the formation of a shear band around the pile shaft. Basu *et al., (*2010) assert that the thickness of the shear band is in the range of 5 to 20 times D_{50}. This scale effect has minimal impact on results when the ratio between the pile diameter and the soil D_{50} is greater than 40-50 (Fioravante, 2002). Additional scale effects typical of calibration chamber testing, (in which stresses are enhanced by applying vertical stresses to the external surfaces of the model), are due to chamber boundary conditions (Bolton *et. al.*, 1999) and to the stress profile created in the calibration chamber that differs from that of the prototype. The latter effect does not occur in the centrifuge owing to the enhanced body forces exerted by the increased g-level.

Foray (1991) performed calibration chamber testing on the installation of jacked piles. The soil stresses induced in the soil mass due to the pile penetration were measured via stress sensors placed in the soil at 3.5 diameters from the model pile. The peak stress was recorded when the pile tip was above the sensor and the stress paths followed by the soil during subsequent loading also indicated that the stresses were similar to those induced around an expanding cavity. The penetration mechanism was also studied by White and Bolton (2004) in a calibration chamber with viewing windows. The displacement field observed resembled that of the expansion of a cavity in the soil. The mechanism of pile penetration is more complicated than the simple expansion of a spherical cavity; nevertheless, cavity expansion theory can be used in order to estimate of stresses existing below the pile base. Several other authors have also made the comparison between the mechanism of pile penetration and that of cavity expansion at the pile base (Randolph *et al.*, 1994, Salgado, 1997, Bolton *et al.*, 1999) but the current literature lacks clear comparisons between the stresses that can be inferred from cavity expansion theory and those measured in experiments. The behaviour of the soil around the pile shaft, which is subjected to substantial shear and particle rearrangement is more complicated than that near the base. The prediction of stresses along the pile shaft is not discussed in this paper. The comparison of the stress field measured below the pile tip during its installation with

that predicted from cavity expansion theory is vital to assess whether this theory can be used to predict loadings on adjacent piles and structures during pile jacking.

The locked-in stresses surrounding driven piles contribute to a significant increase in soil stiffness and hence enhance the pile capacity at working displacements. Piles are often used either in pile groups under structures or as piled walls for earth-retaining purposes. The stress changes imposed in the soil during the installation process of any given pile thus also may have a substantial effect on the capacity of nearby piles. This paper will endeavour to assess the stress state imposed within the soil around monotonically jacked closed ended cylindrical piles through both experimental data and theoretical analyses.

2. Past measurement of soil stress increments due to pile installation

The measurement of stresses in a soil is a non-trivial problem. An accurate stress sensor requires the same stress-strain behaviour as the soil it is embedded in in order to avoid distortion of the stress field that it is trying to measure. Weiler and Kulhawy (1982) listed a series of factors that affect soil measurements and that must be taken into consideration when commercial stress sensors are used including soil type, density, soil stiffness and stress history. Even if all these parameters are taken into account, the accurate design of a conventional stress sensor with these characteristics is impossible due to the unknown behaviour of the soil prior to the measurement and the changing stiffness of soil during any given loading process.

The most common type of stress sensors used both in the field and in the laboratory are diaphragm cells in which the measurement occurs via the deflection of a thin diaphragm attached to a stiff case. Resistance foil strain gauges are used to detect the deflection incurred which can be correlated back to the applied stress. Literature on stress measurements using these sensors shows that diaphragm cells under-estimate the applied soil stresses if they are calibrated based on pressures applied using a fluid, and also show hysteretic behaviour that is difficult to discount using a conventional calibration factor. According to Weiler and Kulhawy (1982), the main sources of errors are due to the stiffness of the sensor relative to the soil and to the limited deformation of the stress sensor causing soil arching around the membrane.

When the membrane deflects, the soil stresses are redistributed around the membrane; in the middle of the membrane, where the deformation is higher, the soil stresses will be lower. An infinitely stiff membrane could measure the soil stresses accurately, but as its deflection would be zero, a conventionally designed cell would also have no output. Weiler and Kulhawy (1982) demonstrated that a percentage of lateral stresses may also be measured as normal stress by the membrane if the ratio between the cell thickness and its diameter is greater than 20%.

Many researchers have attempted to measure soil stresses using diaphragm cells (Chow, 1996; Lehane, 1992; Lehane *et al.*, 1993; White and Lehane, 2004; Zhu *et al.*, 2009; Jardine *et al.* 2013). The majority of these were made with sensors embedded in the pile surface to measure the stress at the interface between the pile and the soil. In this case, the unwanted deflection of the diaphragm results in under-registration of stresses.

Jardine *et al.* (2013) also measured the stress changes within the soil mass caused by pile jacking. An array of commercially available strain-gauged stress sensors was placed at different radii from the pile centreline to measure soil stress changes at various locations. The sensors show a highly hysteretic behaviour during calibration (Zhu *et al.*, 2009) that differs with their previous loading history. The authors establish a calibration factor as an exponential fit of the data normalised. The authors performed the tests in calibration chamber whereby the stresses were increased by means of surcharge bags. A realistic stress profile in the model cannot be reproduced in a calibration chamber and therefore centrifuge testing of pile installation is more appropriate. The use of sensors that necessitate a different calibration factor in loading and unloading can also lead to confusion if the stress paths are unknown beforehand.

Measurements of soil stresses in the field were performed by means of adjacent piles by Lehane (1992) and Chow (1996). The stresses measured may not be the same as those induced in the soil at that location if the measurement pile was not present. As seen by Weiler and Kulhawy (1982), the relative stiffness between the soil and the inclusions changes the stress field around the gauges.

This paper presents the horizontal stress changes caused by jacked pile installations in dry sand in the geotechnical centrifuge. The use of the centrifuge allows the authors to have a realistic stress profile while the use of the null gauges for the measurement of stresses is necessary in order to eliminate membrane deflection.

3. Null gauge technology

Talesnick (2005) developed new sensors for the measurement of soil stresses on a structural boundary. The concept of the sensor, referred to as a 'null gauge', (NG), relies on achieving zero diaphragm deflection by balancing the stresses on the two sides of the diaphragm. The sensor is composed of a stainless steel diaphragm to which a full bridge configuration of high resistance (5000Ω) strain gauges is bonded. The membrane is sealed into a housing and the outer face of the diaphragm sits flush with the soil/structure boundary. An air pipe is inserted into the housing and connected to an electro-pneumatic control valve. When a pressure is applied on the outer surface of the diaphragm, the strain gauge bridge records a voltage change. Through a PID (Proportional Integral Derivative) control loop implemented in Labview (National Instruments), the air pressure necessary to bring the membrane to its underformed shape is applied within the housing. Figure 1 shows a block diagram explaining how the control loop was implemented and an image of the null gauges used for the experiments. In the centrifuge experiment the control loop runs at a frequency of 30 Hz and is activated when the membrane deflection exceeds that caused by a 0.5kPa threshold pressure. When this condition is satisfied, the control loop, via the electro-pneumatic control valves, adjusts the air pressure applied in the membrane housing such that it equates the outer soil pressure. Control testing with soil has illustrated that the diaphragm deflection at any instant of time may thus be assumed to be negligible, theoretically resulting in an infinitely stiff sensor, and that no arching hence occurs. The result is a 1:1 ratio between null pressure and control pressure applied to the membrane through soil (Talesnick 2005, Talesnick *et al.*, 2014). A similar concept has proven reliable for the measurement of normal pressures within a soil mass (Talesnick, 2013). The maximum error in the measurement therefore corresponds to the threshold defined in the control loop divided by the pressure applied in the membrane. This error is less than 5% for pressures larger than 10kPa.

Talesnick (2005, 2013) shows a comparison between the response of commercially available stress sensors and the null gauges. Commercial sensors exhibit a highly hysteretic response when subjected to loading and unloading due to the interaction between the sensor and the surrounding particles. Null gauges exhibit a linear response with almost zero hysteresis.

A potential error in measuring stress also exists if only a small number of particles contact on the sensor diaphragm. The null gauges used on the pile had a sensing diameter of 6 mm and those in the soil a diameter of 12.5 mm. The sensing diameter is thus greater than 20 times the D_{50} size for all sensors. Talesnick *et al.,* (2014) demonstrated from tests with a variety of particle sizes that this is sufficient to obtain reliable measurements with the null gauge method ().

4. Experimental programme

The experimental work presented in this paper was carried out using the 10 m beam centrifuge at Cambridge University (Schofield, 1980). Two model piles were developed for the testing, a square pile and a cylindrical pile. The square pile was used as a measurement pile while the cylindrical pile was jacked at various horizontal distances from it.

4.1 Model piles

4.1.1. Square pile

A square pile and five null gauges were produced at the Technion-IIT. Two were designed to be placed within the soil (shown in Figure 1) and three along the pile shaft (pile null gauges hereafter). The pile comprises a 20 x 20 mm square-section aluminium (AL2024) bar, 213 mm long, with a cavity machined inside to place the pile null gauges. The pile null gauges were made of stainless steel and were mounted with their diaphragms flush with the pile side at distances from the pile tip of 27.5 mm, 52.5 mm and 102.5 mm to the gauge centre. Figure 2 shows a cross section of the pile and a photo of the completed pile. The 20 mm pile width is 64 times the D_{50} size of the sand used, sufficiently large to neglect the scale effects demonstrated by Bolton *et al.* (1999) and Fioravante, (2002) as discussed earlier.

4.1.2 Cylindrical pile

The cylindrical pile consists of a stainless steel tube, 200 mm long, with an outer diameter of 12 mm and an inner diameter of 10 mm. The pile dimensions were chosen to resemble a typical onshore pile when tested at 50g in the centrifuge. Dimensions scale linearly with the g-level, resulting in the prototype pile being 10 m long and having a diameter of 0.6 m. The bending stiffness of the model pile is higher than that of an equivalent prototype in order to avoid pile buckling during installation. The pile was closed at its toe by means of a load cell instrumented with strain gauges arranged in full Wheatstone bridge to minimise temperature effects. The strain gauges were glued on the internal side of the tip. The head load is recorded at the pile head with an external load cell. The pile diameter is 38 times the D_{50} size of the sand used, sufficiently large to neglect the scale effects demonstrated by Bolton *et al.* (1999).

The side surface of the pile was made rough by sticking sand grains to it with epoxy. The roughness of the pile was measured by means of a profilometer and, following the definition by Uesugi and Kishida (1987), the normalised roughness R_N was calculated and found to be 0.15. According to Porcino (2003), the coefficient of friction between the sand and the interface is independent of the interface roughness for $R_N > 0.06$; the interface friction angle obtained in the current centrifuge testing is therefore independent on the shaft surface roughness and should correspond to fully rough behaviour.

4.2 Sand properties

Marine Quartz sand produced by Specialist Aggregates Ltd, UK was used for the experiment. The sand is poorly-graded (C_U = 1.88) with a rounded grain shape that makes it ideal for laboratory testing. The sand has a D_{50} of 312 μm and the maximum and minimum voids ratios are 0.972 and 0.577 respectively.

4.3 Test overview

The centrifuge modelling described in this paper involved testing of a 1:50 scale model pile at a centrifugal acceleration of 50g. This implies that the stresses and strains in the model and prototype are identical at homologous locations. In order to interpret other quantities within the

model to prototype scale, scaling laws are used which are fully described by Taylor (1994). In this paper all results will be presented at prototype scale.

The centrifuge model tested comprised a uniform sand layer within an 850 mm diameter (42.5 m prototype) cylindrical steel model container. Sand was poured into a cylindrical container by means of an automatic robotic sand pourer (Madabhushi *et al,* 2006*)* so as to achieve a uniform sand layer at a relative density of 86%. The pouring was paused when the thickness of the sand layer was 195 mm (9.75 m prototype) for the placement of soil null gauge NG-S_{150} and at a thickness of 255 mm (12.75 m prototype) for the placement of the soil null gauge NG-S_{90}. The soil null gauges were pushed into the soil to a depth of half of their diameter with their membrane being perpendicular to the ground surface in order to measure the change in horizontal stress caused by pile jacking. The final orientation was checked with a miniature spirit level. The placement procedure is shown in Figure 3 (a) and the location of the soil null gauges is shown in Figure 4. The final sand thickness was 345 mm and the depths of the null gauges 150 mm and 90 mm respectively.

In order to minimise soil stress changes due to installation of the measurement pile, the square pile was installed prior to flight. The installation of the pile was made in the centre of the container by means of an automatic actuator (Haigh *et al*, 2010) until the pile tip reached a prototype depth of 10 m. Figure 3 (b) shows the square pile while installed. The pile was oriented such that two of the pile null gauges were facing the soil null gauges; the other pile null gauge was on the opposite side of the pile shaft. Figure 4 shows the location of the square and the cylindrical pile relative to the soil null gauges.

The cylindrical pile was installed in flight using the automatic actuator to a final prototype depth of 10 m. All installations were executed at an equivalent prototype rate of 10 mm/s with data acquired at 4Hz. The first installation (I-1) was performed mid-way between the soil null gauges and the pile null gauges. Following the first installation, the pile was removed and then moved to a different location while the g-level was kept constant. Four additional installations (I-2 to I-5) were performed in the same manner at a minimum centre-to-centre distance of 3*D*, as shown in Figure 4. All installations occurred along the line joining the measurement pile and soil gauges.

The installation of each pile causes soil disturbance in the area where the pile is installed: following pile removal the soil density in that area may be different from before the installation. The stresses measured by the null gauges after the first installation could be biased by the change in soil density due to the previous installations. Nevertheless it will be shown in the following paragraph that the results of the five installations can be compared.

5. Results and interpretation

5.1 Base and shaft load

The average shaft load is the difference between the head and the base load measured by means of the load cells presented in Section 4.1.2. During installation I-3, the actuator was stopped early due to proximity to the square pile, the size of its cap being greater than the distance between the two piles. Figure 5 shows the base and shaft load for the five installations (I-1 to I-5) and their average value. The maximum value of base load is 4.85 kN while the maximum shaft load is 0.9 kN. The shaded region indicates a range of ±20% of their average value. All curves lie within the region and there is no clear correlation between their values at a certain depth and the order of the installation. Results of the five installations can therefore be compared both in terms of base and shaft behaviour as there is no correlation between the pile installation sequence and variations in the pile installation loads.

5.2 Data normalisation

Normalisation of data is necessary in order to better compare the readings of the null gauges. Prior to the installation, the soil null gauges have a non-zero value due to the geostatic stresses in the soil. In a similar manner the pile null gauges record an initial pressure; these pressures, if normalised by the vertical pressure at the depth of the gauge, are higher than the pressures recorded by the soil null gauges. Higher pressures are expected when stiff inclusions are immersed in a soil medium.

The following sections illustrate the horizontal stress changes recorded during each pile installation. In each case the pressure recorded by the sensor prior to installation is subtracted

from the current reading. In this way, only the horizontal stress increments ($\Delta\sigma_h$) due to the installation are considered. For comparison purposes, increments of pressure have been normalised by the pile base pressure at the particular depth of penetration.

Pile penetration is presented as the change in vertical distance between the pile tip and the sensor, (*h),* normalised by the pile radius, (*R*). For *h/R*<0 the pile tip is above the sensor, for *h/R*=0 the pile tip is aligned horizontally with the sensor, and for *h/R*>0 the pile tip has passed the sensor. This form of normalisation allows results from different gauges to be compared in a single graph.

5.3 Horizontal stress increments caused by jacked pile installation

5.3.1 Pile installation equidistant from square pile and soil null gauges

Installation I-1 was performed mid-way between the soil null gauges and the pile null gauges at a horizontal distance *x* of around 9*D*. The horizontal distance is calculated as the distance from the pile centreline to the outer face of the gauge.

Figure 6 shows the relationship between the ratio of the increment of horizontal stress ($\Delta\sigma_h$) and the pile base stress (q_b) versus the normalised depth of the pile tip (*h/R*). The maximum value of horizontal stress increment at 9*D* from the pile is 0.5% of the base resistance. Maximum changes in horizontal pressure occur when the pile tip is slightly above sensor level (i.e. *h/R*<0), the distance below the pile tip at which the maximum stress is measured is greater at shallower depths of penetration. The values are similar to those recorded by Jardine *et al.* (2013) at the same distance during installation of a cylindrical pile in a calibration chamber.

It can be seen that the peak pressures recorded by gauges on the measurement pile are substantially higher than those recorded within the soil. The over-registrations are 80% and 100% for null gauges C and B respectively. If instrumented piles are to be used to measure the stress changes caused by the installation of a pile nearby, a substantial over-registration must be expected due to their stiffness. This also implies that the benefit to the stiffness and capacity

of nearby piles owing to stress changes due to subsequent pile installation may be enhanced by a similar amount.

5.3.2 Variation of stress changes at horizontal distances from pile centreline

Figure 7 (a) to (d) shows the horizontal stress increments divided by the base resistance at different horizontal distances from the pile axis. Installations I-2 to I-5 are included in the plots. The axis scale changes between the four subplots in order to better show the stress variation across the four gauges as a function of distance.

At all distances the stresses measured on the measurement pile are larger than those measured in the soil mass. This discrepancy becomes less evident at large distances from the pile, where soil movements are less restricted by the solid inclusion, the ratio between the diameter of the inclusion and the radius from the pile having reduced.

From Figure 7 (a) to (d) it can also be seen that the increase in the horizontal stress normalised by the base pressure is different for the two soil null gauges; the deeper gauge NG-S_{150} shows smaller normalised increases in stress compared to the shallower NG-S_{90}. The same is not valid for the pile null gauges. This may be related to the lower dilatancy of granular soils at higher stresses and hence depths (Bolton, 1986).

6. Comparison with Boussinesq theory

A quick and simple prediction of the stress field around the pile can be made by considering the Boussinesq closed-form solution for linear elastic soil. The analytical solution was developed for shallow foundations and is therefore different from the mechanism around an embedded pile base as it implies zero vertical stress being applied on a plane level with the pile base. Nevertheless, the method is still one of the most commonly used concepts in geotechnical engineering. Stresses are calculated via equilibrium equations and are therefore less subject to errors compared to strains.

For a uniform circular pressure, Alhvin and Ulery (1962) published a detailed tabulation of the stresses with depth at a given horizontal distance (x) from the centreline of a uniformly loaded circular foundation. Figure 8 shows the comparison for x/R=5 (a) and x/R=10 (b).

The curves follow the same trend; larger differences being present just below the pile tip owing to the boundary condition error. For the Boussinesq solution, the shallow soil at a horizontal distance from the pile is not loaded vertically owing to the presence of the ground surface and consequently horizontal stresses are small. For the pile, the boundary conditions at the foundation depth are different from the Boussinesq solution as the soil is sheared by the presence of the shaft and confined by the soil above.

The Boussinesq solution under-estimates the recorded horizontal stress up to a maximum of 52% at x/R = 5 and 40% at x/R = 10. Nevertheless, if horizontal stress measurements are not available, the Boussinesq distribution could be used as a first estimate of stresses. Taking into consideration the under-estimation shown above, it would give a conservative prediction of enhancement of the capacity of nearby piles and could be used with a factor of two to give conservative estimates of the pressure applied to a nearby retaining structure.

7. Prediction of increment of radial stresses using spherical cavity expansion

For closed-ended piles, Randolph *et al.*, (1994) proposed the analogy between the expansion of a spherical cavity and the bearing failure. Whilst the true deformation mechanism below a pile is obviously more complicated than this, involving substantial shear, spherical cavity expansion does allow an analytical prediction of stresses around a pile tip to be made. For jacked piles the soil below the pile tip is highly compressed and the stresses are such as to cause significant particle breakage (White and Bolton, 2004). If the particles are reduced in size it is expected that the soil mechanical properties will also be changed. The cavity expansion method, in its current form, is not able to predict such a variation.

The closed form cavity expansion solution is based on the assumption that the soil beneath the pile tip is at its ultimate state. The calculation of the stress distribution around the cavity can be

made using the expressions of Carter *et al.* (1986) or Yu & Houlsby (1991); both assume that the soil behaves as an elastic-perfectly plastic material and that the failure occurs with a Mohr-Coulomb criterion at constant rate of dilation.

The solution by Yu & Houlsby (1991) is compared in this paper with the readings from the null gauges when the pile tip is located at 78 mm depth. This choice was made for two reasons; firstly, at that depth NG-S_{90} records its maximum value and secondly, all sensors could be included in the comparison. The soil is modelled as linear elastic-perfectly plastic with the yield criterion being non-associated Mohr Coulomb.

The null gauges are able to record only stresses orthogonal to the membrane, horizontal in the test, so it is necessary to project the measured stresses along the radial direction of the spherical cavity. Considering that the sensors are within the plastic region, the stress component radial to the cavity sphere (σ_1) can be computed from the Mohr's circle at failure, giving:

$$\sigma_1 = \frac{\sigma_h}{\frac{1+K_a}{2} - \frac{1-K_a}{2}\cos(2\vartheta)} \qquad [1]$$

Figure 9 shows the stress projection scheme used. The angle θ is different for the four gauges and is computed according to Equation 2.

$$\theta = \tan^{-1}(x/h) \qquad [2]$$

Figure 10 shows the comparison between radial stress increments (in spherical coordinates) ($\Delta\sigma_1$) predicted by cavity expansion analysis using an angle of friction $\varphi' = 30°$ and that measured during the centrifuge test and projected into the radial direction using equation 1. The distance from the centre of the expanding cavity is termed r. $r / R = 1$ is hence representative of the conditions at the spherical cavity wall, at which the pressure is computed as the mean stress under the pile:

$$p = \frac{q_b(1+2K_a)}{3} \quad [3]$$

The angle of friction φ′=30° is the residual friction angle measured in a consolidated drained test of Marine Quartz sand prepared at 86% relative density tested at initial effective stresses of 100, 200 and 300 kPa.

The prediction shows good agreement with the experimental data. The maximum error is recorded for the pile null gauges (empty markers) that, as stated in the previous section, record higher stresses compared to their equivalent in the soil due to the pile stiffness. The analytical solution provides an excellent fit to the data measured by the null-gauges in the soil at all radii, with an R^2 value for the correlation of 0.983 being obtained. More experimental data is necessary for $5< r / R < 12$ in order to assess the applicability of the analytical solution at these radii.

In conclusion, spherical cavity expansion could be used to give a good estimate for radial stress increments induced by pile jacking.

8. Conclusions

This paper describes the stress fields measured during the installation of jacked piles in sand. Stress changes during the installation are measured accurately by means of null gauges that, contrary to conventional stress sensors, are unaffected by the soil stress history and membrane deflection.

Measurements are made both by null gauges mounted on a square pile (pile null gauges) and by null gauges placed within the soil (soil null gauges) at the same distance during pile installation. Results show that when the pile is at equal distance between the pile null gauges and the soil null gauges, higher stresses are recorded on the pile due to its stiffness. The discrepancy is less evident at large distance where soil movements are less restricted by the solid inclusion.

Prediction of the stresses along the pile via the Boussinesq solution results in similar trends, with larger discrepancies for low values of *h/R* due to the different boundary conditions. At depths greater than one pile diameter the Boussinesq solution returns a similar trend to that measured in the centrifuge, but slightly underestimates applied stresses.

Prediction of stresses by spherical cavity expansion shows a good estimate of the stresses measured by the soil null gauges.

Results are relevant for the installation of a pile in the vicinity of an existing pile. Residual stresses induced by the installation of a single pile must be considered. Furthermore, when in-soil stresses are measured by means of an instrumented pile, the over-registration due to the stiffness of the pile must be considered.

Acknowledgements

The Authors would like to acknowledge the efforts of Mr. M. Ringle of the Technion – IIT for the design and production of the square pile. The research was funded by Giken Ltd. and the Coleman-Cohen Exchange Programme to whom a great acknowledgement is addressed.

References

Ahlvin, R.G. and Ulery, H.R. (1962). Tabulated values for determining the complete pattern of stresses, strains and deflections beneath a uniform load on a homogeneous half space. *Highway Research board, Bulletin 342*

Basu, P., Loukidis, D., Prezzi, M. and Salgado, R. (2010). Analysis of shaft resistance of jacked piles in sands. *International Journal for Numerical and Analytical Methods in Geomechanics, John Wiley & Sons, Ltd* **35**: 1605-1635

Bolton, M.D. (1986).The strength and dilatancy of sands. *Géotechnique* **36(1)**: 65-78

Bolton, M.D., Gui, M.W., Garnier, J., Corte, J.F., Bagge, G., Laue, J. and Renzi, R. (1999). Centrifuge cone penetration tests in sand. *Géotechnique* **49(4)**: 543-552

Carter, J.P., Booker, J.R. and Yeung, S.K. (1986). Cavity expansion in cohesive frictional soils. *Géotechnique* **36(3)**: 349-358

Chow, F.C. (1996). Investigations into the behaviour of displacement piles for offshore foundations. *PhD thesis,* Imperial College of Science, technology and Medicine, London

Fioravante (2002). On the shaft friction modelling of non-displacement piles in sand. *Soils and Foundations* **42(2)**: 23-33

Foray, P. (1991). Scale and boundary effects on calibration chamber pile tests. *First International Symposium on Calibration Chamber Testing, Potsdam, New York. Elsevier* pp.147-160

Haigh, S.K., Houghton N.E., Lam, S.Y., Li, Z. and Wallbridge, P.J. (2010). Development of a 2D servo-actuator for novel centrifuge modelling. *Physical Modelling in Geotechnics – Springman, Laue & Seward (eds)* Taylor & Francis group, London

Jardine, R.J., Zhu, B.T., Foray, P. and Yang, Z.X. (2013). Measurement of stresses around closed-ended displacement piles in sand. *Géotechnique* **63(1)**: 1-17

Ko, H.Y., Atkinson, R.H., Goble, G.G. and Ealy, C.D. (1984). Centrifugal modelling of pile foundations. *Analysis and Design of Pile Foundations ASCE* pp-21-40.

Lehane, B.M. (1992). Experimental investigations of pile behaviour using instrumented field piles. *PhD thesis,* Imperial College of Science, technology and Medicine, London

Lehane, B.M., Jardine, R.J., Bond, A.J. and Frank, R. (1993). Mechanisms of shaft friction in sand from instrumented pile tests. *Journal of Geotechnical Engineering ASCE* **119(1)**: 19-35

Madabhushi, S.P.G., Houghton, N.E. and Haigh, S.K. (2006). A new automatic sand pourer for model preparation at University of Cambridge. *Physical Modelling in Geotechnics-6th ICPMG '06,* Taylor & Francis group, London

Porcino, D., Fioravante, V., Ghionna V.N. and Pedroni S. (2003). Interface behaviour of sands from constant normal stiffness direct shear tests. *Geotechnical Testing Journal* **26(3):** 1-13

Poulos, H. (1987). Analysis of residual stress effects in piles. *Journal of Geotechnical Engineering ASCE* **113(3)**: 216-229

Randolph, M.F., Dolwin, J. and Beck, R. (1994). Design of driven piles in sand. *Géotechnique* **44(3)**: 427-448

Salgado, R., Mitchell, J.K. and Jamiolkowski, M. (1997). Cavity expansion and penetration resistance in sand. *Journal of Geotechnical and Geoenvironmental Engineering,* April pp.344-354.

Schofield, A.N. (1980). Cambridge Geotechnical Centrifuge Operations. *Géotechnique* **30 (3)**: 227-268

Taylor, R.N. (1994). Geotechnical Centrifuge Technology. *Blackie Academic & Professionals*, Taylor & Francis Group, London.

Talesnick, M. (2005). Measuring soil contact pressure on a solid boundary and quantifying soil arching. *Geotechnical Testing Journal* **28(2)**

Talesnick, M. (2013). Measuring soil pressures within a soil mass. *Canadian Geotechnical Journal*, **50**(7): 716-722.

Talesnick, M., Ringel. M and Avraham, R. (2014). Measuring of contact soil pressure in physical modelling of soil-structure interaction. *International Journal of Physical Modelling in Geotechnics*, **14**(1): 3-12.

Uesugi, M. and Kishida, H. (1987). Tests of the interface between sand and steel in the simple shear apparatus. *Géotechnique* **37 (1)**: 45-52

Weiler, W.A. and Kulhawy, F.H. (1982). Factors affecting stress cell measurement in soil. *Journal of the Geotechnical and Foundation Division, ASCE* Vol.108, No. GT12, pp.1529-1548

White, D.J. and Bolton, M.D. (2004). Displacement and strain paths during plane-strain model pile installation in sand. *Géotechnique* **54(6)**: 375-397

White, D.J. and Lehane, B.M. (2004). Friction fatigue on displacement piles in sand. *Géotechnique* **54(10)**: 645-658

Yu, H.S. and Houlsby, G.T. (1991). Finite cavity expansion in dilatant soils: loading analysis. *Géotechnique* **41(2)**: 173-183

Zhu, B., Jardine, R.J. and Foray, P. (2009). The use of miniature soil stress measuring cells in laboratory applications involving stress reversals. *Soils and foundations* **49(5)**: 675-688

Figure captions

Figure 1. Block diagram and photo of null gauge technology

Figure 2. Cross section and photo of the instrumented square pile

Figure 3. Model preparation sequence: (a) null gauge positioning (b) installation of square pile

Figure 4. Installation sequence and side view of centrifuge model

Figure 5. (a) Base and (b) shaft load recorded during installations I-1 to I-5

Figure 6. Increment of pressure normalised by the base resistance measured for the pile installed at the same distance between soil null gauges and pile null gauges

Figure 7. Increment of pressure normalised by the base resistance measured for the pile installed at horizontal distances from soil null gauges and pile null gauges

Figure 8. Comparison between the Boussinesq solution for stresses beneath a uniformly loaded circular foundation and the measured increment of pressure below the pile tip during penetration

Figure 9. Stress projection scheme

Figure 10. Comparison between spherical cavity expansion solution for φ =30° and radial stress increments by all null gauges when the pile tip is at 78 mm depth

Figure 1
Click here to download high resolution image

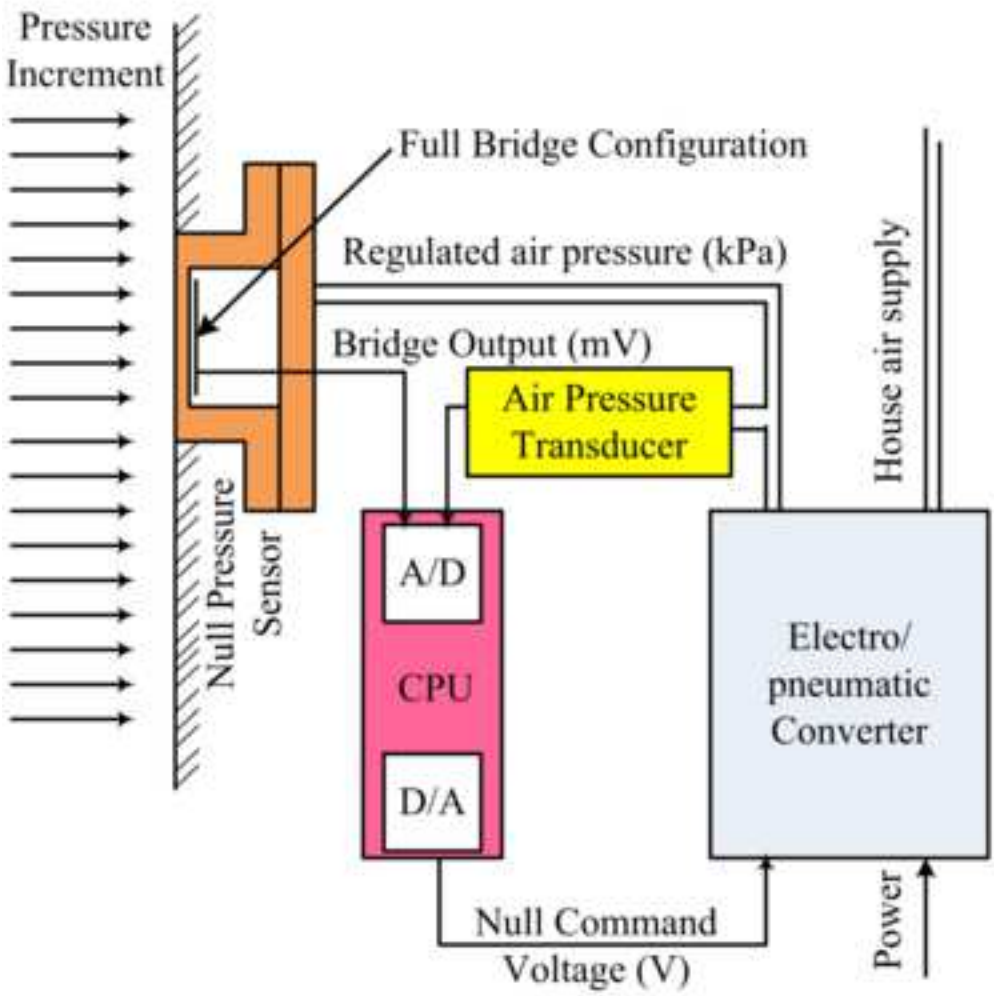

Figure 2
Click here to download high resolution image

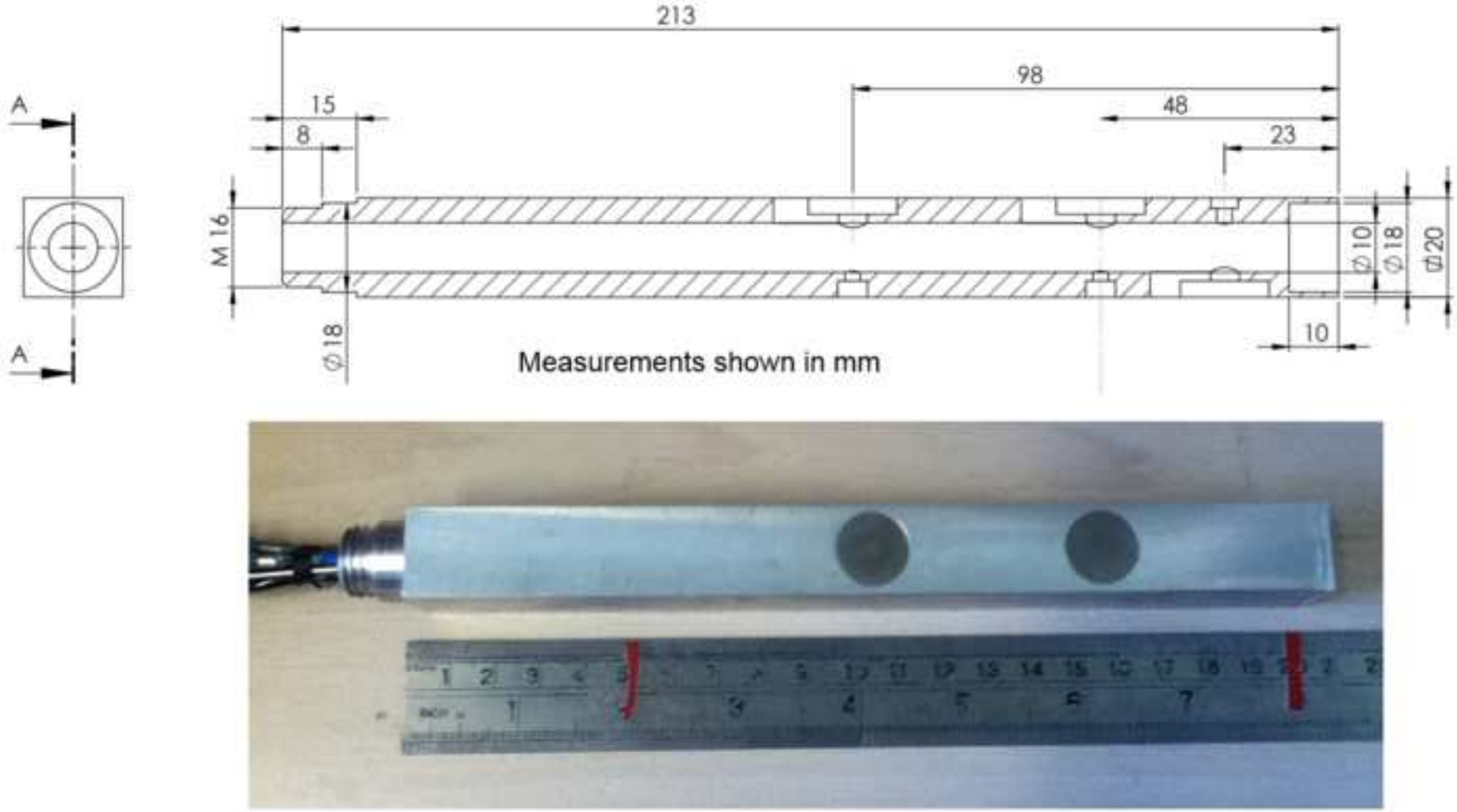

Figure 3b
Click here to download high resolution image

Figure 3a
Click here to download high resolution image

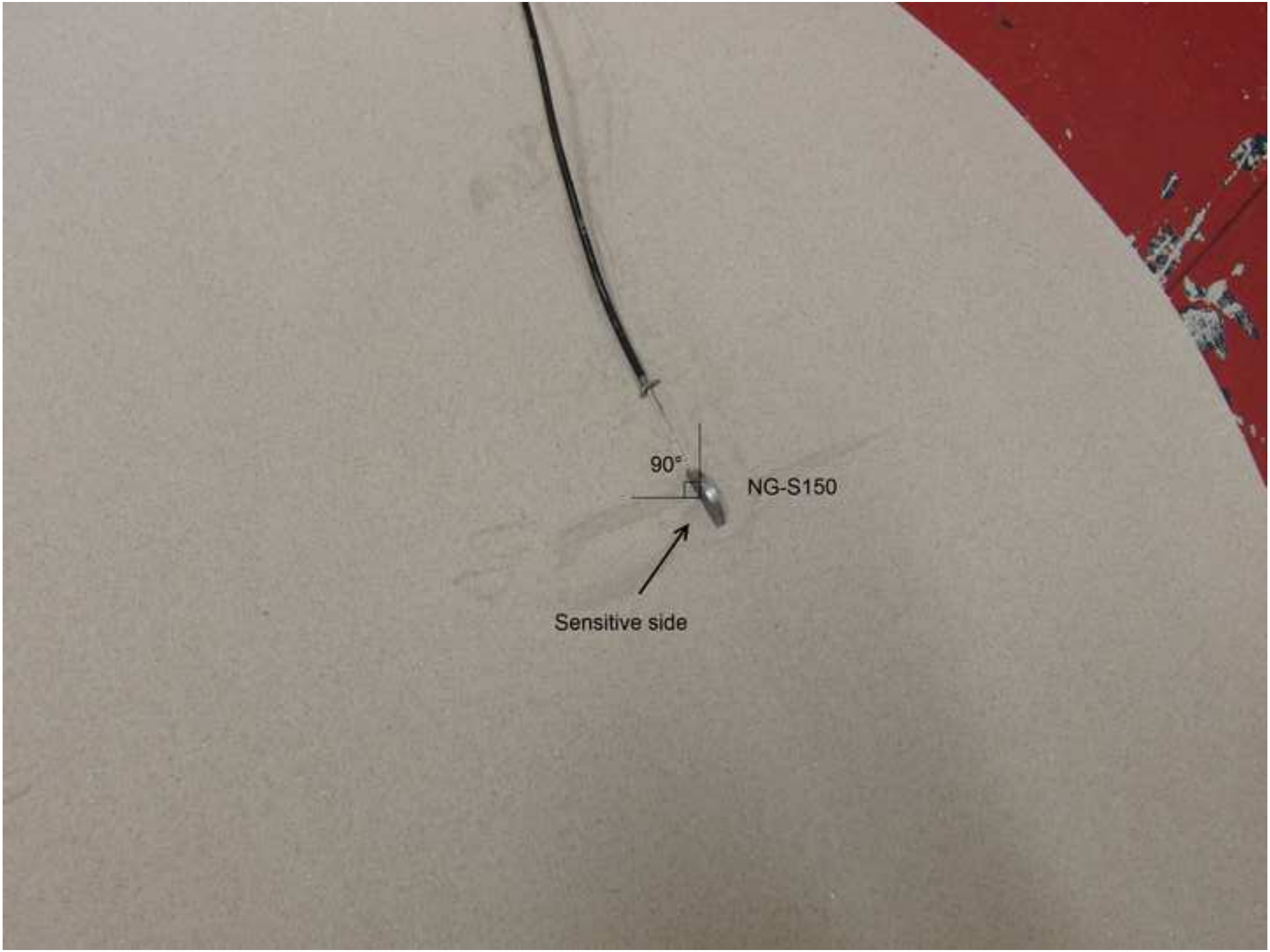

Figure 4
Click here to download high resolution image

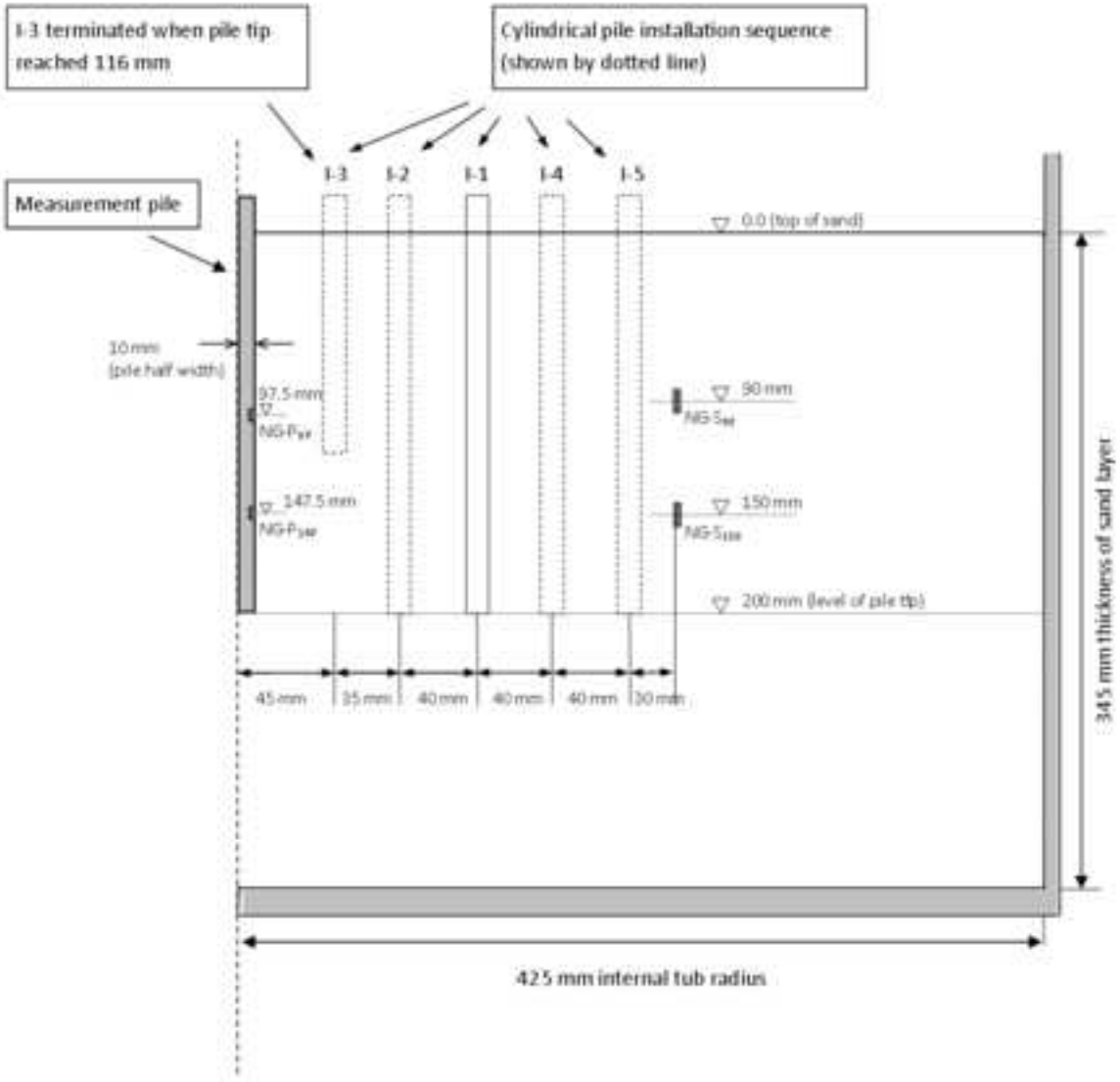

Figure 5
Click here to download high resolution image

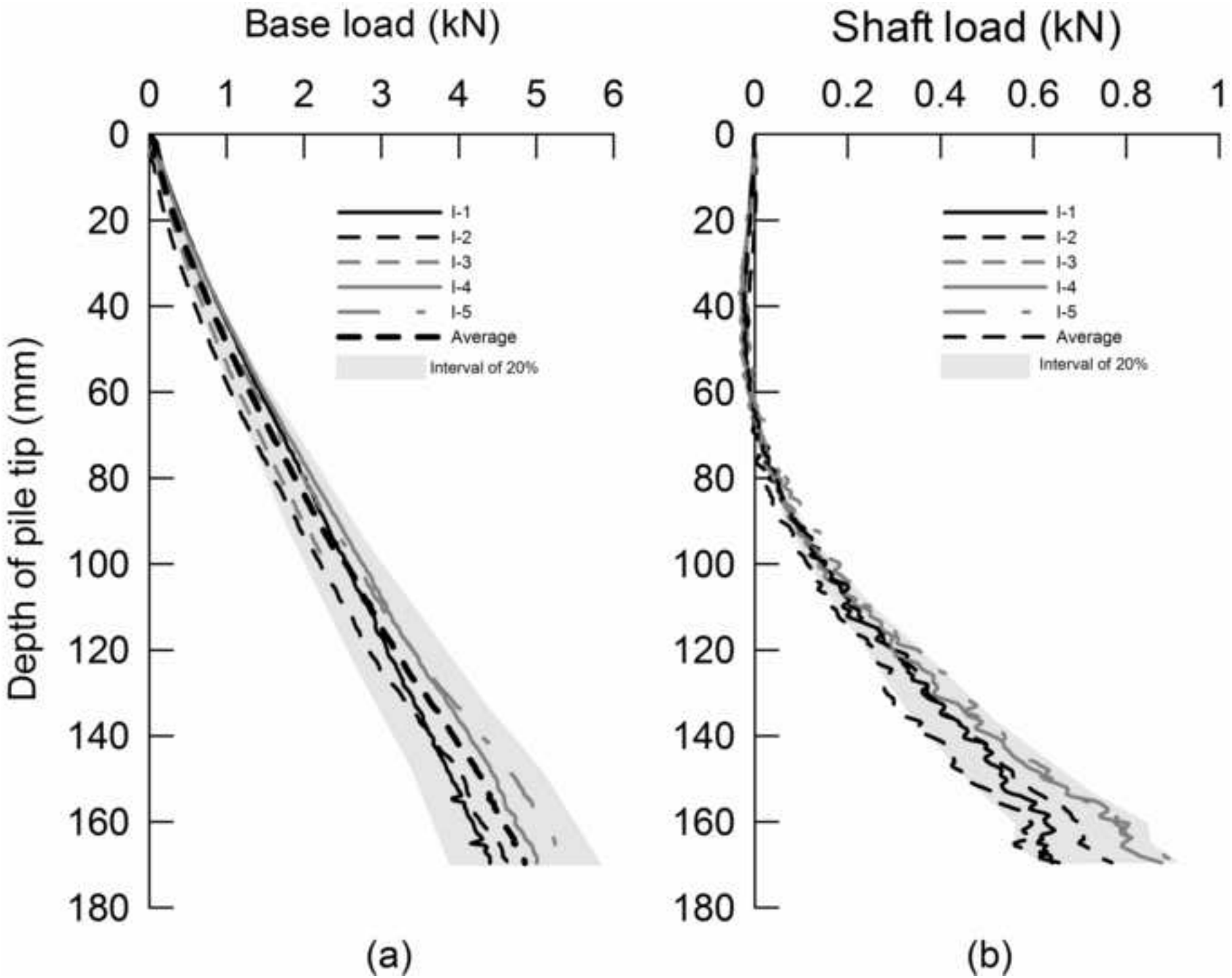

Figure 6
Click here to download high resolution image

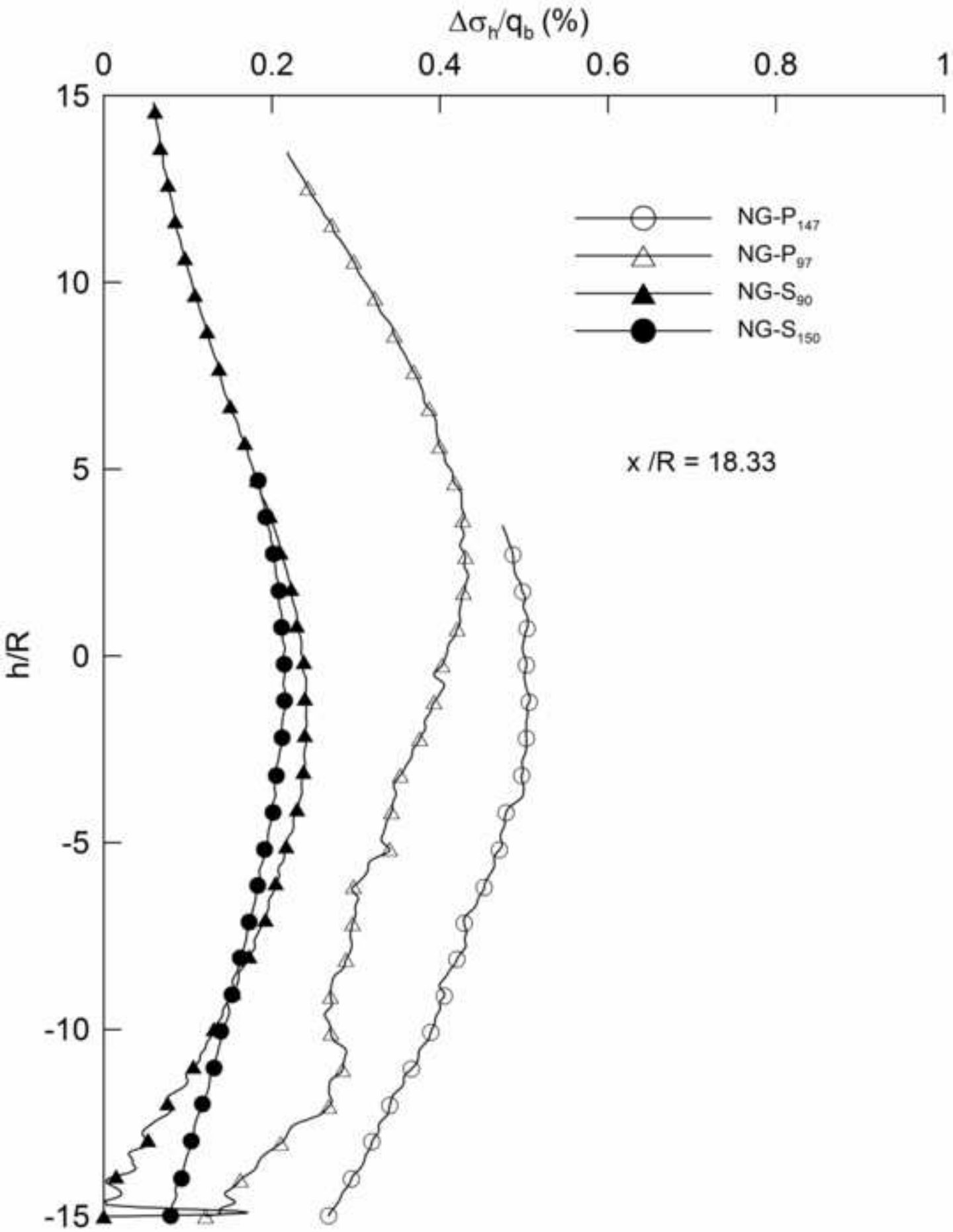

Figure 7
Click here to download high resolution image

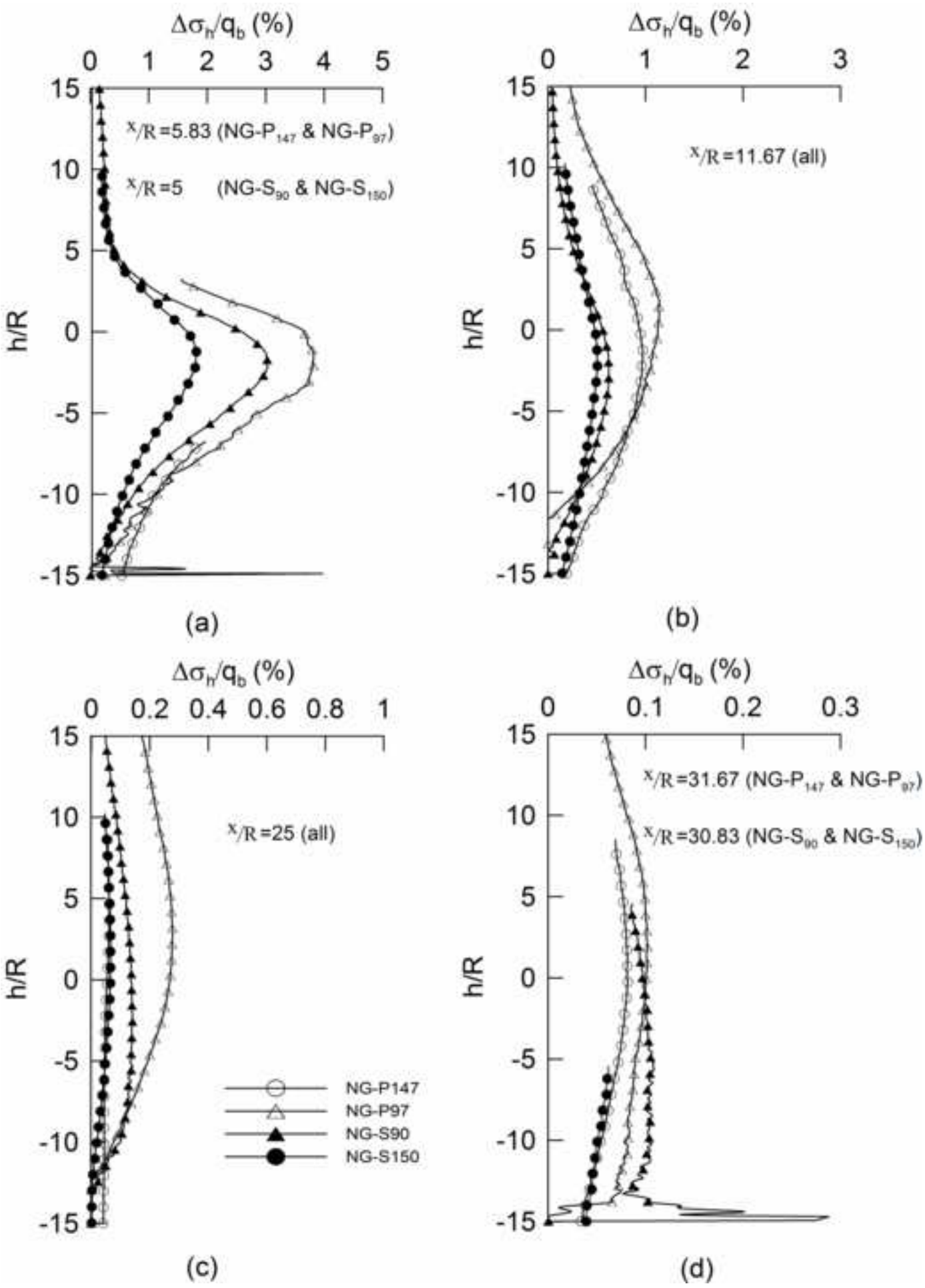

Figure 8
Click here to download high resolution image

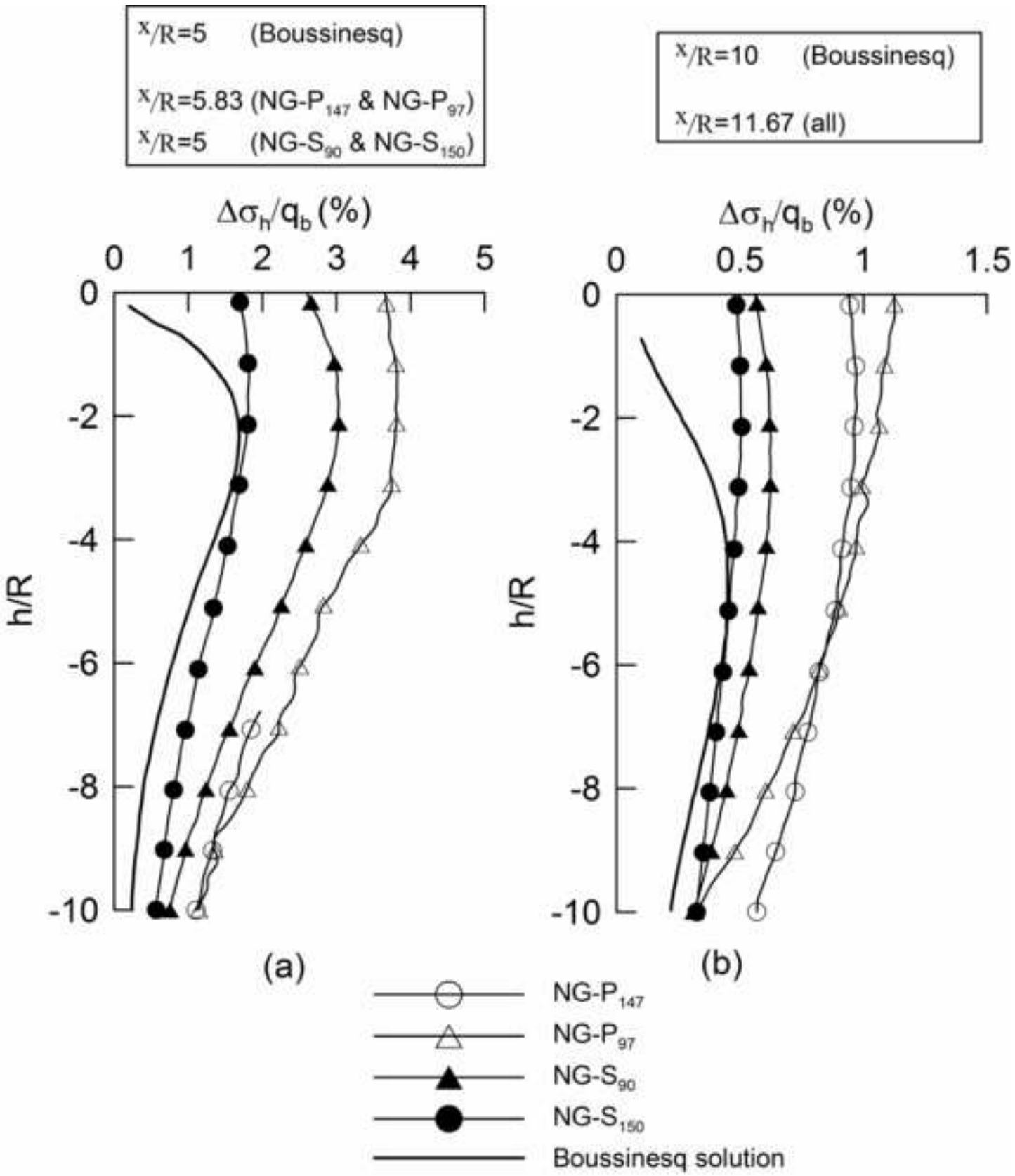

Figure 9

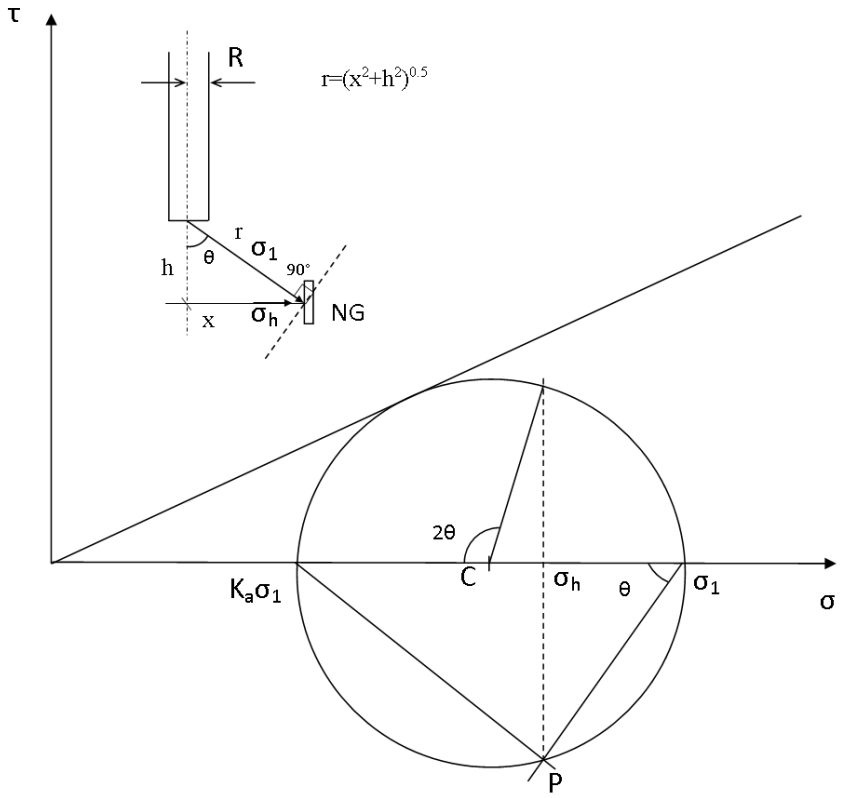

Figure 10
Click here to download high resolution image